Measurement of the direct CP asymmetry in the $B^0 \to K^+\pi^-$ decays

The CDF II Collaboration
URL http://www-cdf.fnal.gov
(Dated: April 10, 2006)

The direct CP asymmetry in $B_d \to K^+\pi^-$ has been measured with 355 pb^{-1} of CDF II data collected between February 2002 and August 2004.

Preliminary Results for Winter 2006 Conferences

I. INTRODUCTION

The CDF II detector can reconstruct significant samples of charmless two–body B decays of interest for the purpose of investigating CP violation [1], by means of a dedicated trigger on impact parameter. While B_d decays are being studied also at leptonic B-factories, the B_s modes are currently unique to the Tevatron.

Experimentally, the mass peaks of all two–body decays of type $B_{d,s} \to h^+h^{'-}$ (where $h, h' = K, \pi$), when reconstructed with a conventional assignment of pion mass to both prongs, are expected to contribute a number of overlapping peaks, seen collectively as a single unresolved bump in the CDF II data.

The current analysis measures the direct CP asymmetry in $B^0_d \to K^+\pi^-$, by exploiting the small kinematics differences between distinct modes and the particle identification information provided by the specific ionization (dE/dx) in the drift chamber. The dE/dx measurement was calibrated with a sample of kaons and pions from $D^{*+} \to D^0\pi^+ \to [K^-\pi^+]\pi^+$ decays. The resulting K/π separation is $\simeq$1.4σ.

II. DATA SAMPLE & EVENT SELECTION

The analysis is performed on a sample corresponding to an integrated luminosity of $\simeq$ 355 pb^{-1} collected with the CDF II detector ([2]) between February 2002 and July 2004. Data were collected by the hadronic B trigger, designed to select events containing track pairs exiting from a common displaced vertex.

The Level 1 trigger is based on the eXtremely Fast Tracker which reconstructs tracks with $p_T > 1.5$ GeV/c in the transverse plane of the drift chamber. The trigger selection requires two opposite charge tracks with $p_T > 2.0$ GeV/c and azimuthal opening angle smaller than 135°.

At Level 2 the Silicon Vertex Tracker performs a high–resolution online track reconstruction in the transverse plane within the silicon vertex detector and allows to select pairs of tracks with impact parameters larger than 100 μm, and transverse decay length larger than 200 μm, which are compatible with the hypothesis of a two-body decay of a long–lived particle.

At Level 3, full event reconstruction is performed by standard reconstruction software running on a farm of commercial CPUs'. Cuts applied at Level 1 and Level 2 are confirmed using offline-quality quantities, and in addition the invariant mass of the track pair is required to be 4.0 GeV/c^2 $< m(pair) <$ 6.0 GeV/c^2.

A. Optimization of analysis cuts

The $B^0_{(s)} \to h^+h^{'-}$ signal is reconstructed by applying a vertex constrained fit to each track pair of the event and confirming the trigger cuts (on transverse momenta and impact parameters of the tracks, and on transverse decay length and impact parameter of the B candidate) using offline quantities. The cuts applied on the following variables:

- impact parameter of the two tracks,
- transverse decay length of B candidate,
- impact parameter of B candidate,
- tridimensional vertex quality χ^2_{3D},
- isolation of the B candidate

particularly effective in reducing the background level, have been optimised by minimizing the figure of merit $\frac{1}{\sqrt{S}}\sqrt{z + w(\frac{B}{S})}$. This new figure of merit is a better parameterisation than the usual $\sqrt{S+B}/S$ to estimate the dependence on S and B of the resolution on the measurement of A_{CP} as determined by the fit. The constants z and w are determined by interpolating a limited number of values of the resolution on A_{CP} determined by the fit applied on simulated samples generated varying S and B. This figure of merit is then used to determine the optimised cuts for the measurement of A_{CP}.
The B isolation is defined as $\frac{p_T(B)}{p_T(B)+\sum p_T}$, where the sum on the transverse momentum is extended to the tracks contained in a cone with radius = 1 in the η-ϕ space around the B meson flight direction. The final values of the cuts are summarized in Tab. II, *top left*.

The resulting $B^0_{(s)} \to h^+h^{'-}$ invariant mass distribution, with pion mass assignment to both decay tracks, is reported in Fig. 1. A clean signal of events is observed. A simple, binned fit with a Gaussian shape for the signal and exponential (combinatorics) plus an Argus (physics) distribution for the background estimates the signal-yield to be 2327 ± 77 events with a standard deviation $\sigma = 39 \pm 1$ MeV/c^2, with an approximate purity of $S/B \approx 6.5$ at peak.

III. LIKELIHOOD FIT

The relative raw $B^0_{(s)} \to h^+h^{'-}$ fractions are measured by an unbinned maximum likelihood fit which combines kinematics and dE/dx information. The discriminating variables used in the fit are:

- $M_{\pi\pi}$ which is the invariant mass of the track pair computed by assigning the pion mass to both tracks;
- $\alpha = (1-\frac{p_1}{p_2}) \cdot q_1$ which is the charge-signed momentum imbalance. p_1 (p_2) is the modulus of the smaller (larger) momentum of the two tracks and q_1 is the charge of the track with smaller momentum. The $M_{\pi\pi}$ dependence on α is computed analytically, the formulas relative to the six signals $B_d \to \pi^+\pi^-$, $B_d \to K^+\pi^-$, $\overline{B}_d \to K^-\pi^+$, $B_s \to K^-\pi^+$, $\overline{B}_s \to K^+\pi^-$, $B_s \to K^+K^-$ show that these two variables provide some separation between particles and antiparticles (see Tab. I);
- $p_{tot} = p_1 + p_2$ which is the scalar sum of the two track momenta;
- $\mathsf{ID1}$ ($\mathsf{ID2}$) which contain the dE/dx information for the track with smaller (higher) modulus of the momentum.

The Likelihood function is $\mathcal{L} = \prod_{i=1}^{nev} \mathcal{L}_i$. The index i runs over the events and the Likelihood of the i^{th} event is:

$$\mathcal{L}_i = b \cdot \mathcal{L}^{bckg} + (1-b) \cdot \mathcal{L}^{sign} \tag{1}$$

The index sig ($bckg$) labels the likelihood term of signal (background), b is the background fraction.

- $\mathcal{L}^{sig}(\vec{\theta}) = \sum_j f_j \cdot pdf_j^{mass}(m_{\pi\pi}|\alpha;\vec{\theta}) \cdot pdf_j^{PID}(\mathsf{ID1},\mathsf{ID2}|p_{tot},\alpha;\vec{\theta}) \cdot pdf_j^{momentum}(\alpha, p_{tot};\vec{\theta})$ is the signal likelihood. The index j runs over the six $B_{d,s} \to h^+h^{'-}$ signal modes shown in Tab. I and the parameters f_j are their relative fractions determined by the fit. pdf_j^{mass}, $pdf_j^{momentum}$ and pdf_j^{PID} are the factors of the likelihood that use the information derived respectively from the kinematics and from particle identification.
  - The mass term is:

$$pdf_j^{mass}(m_{\pi\pi}|\alpha\ ;\ \sigma,\vec{\theta}) = 0.9 \cdot \frac{1}{\sigma_1\sqrt{2\pi}} e^{-\frac{1}{2}\left(\frac{m_{\pi\pi}-\mathcal{M}(\alpha)}{\sigma_1}\right)^2} + 0.1 \cdot \frac{1}{\sigma_2\sqrt{2\pi}} e^{-\frac{1}{2}\left(\frac{m_{\pi\pi}-\mathcal{M}(\alpha)}{\sigma_2}\right)^2}$$

    The pdf of the $m_{\pi\pi}$ variable is the sum of two Gaussians of width σ_1 and σ_2 and centered on $\mathcal{M}(\alpha)$. σ_1 and σ_2 are the floating resolutions of the two components. $\mathcal{M}(\alpha)$ are the analytic functions defined in Tab. I that determine the expected value of $m_{\pi\pi}$ as a function of the momentum imbalance (α).
  - The PID term of the signal Likelihood is extracted through a convolution integral — which accounts for track-to-track dE/dx correlation — and a variable transformation from the dE/dx-residual to the ID variable. dE/dx correlations force us to use a joint p.d.f. for the observed dE/dx residuals of the two tracks: $pdf(res_1^{obs}, res_2^{obs})$. From the $D^0 \to K\pi$ sample we extracted an accurate parameterization of the shapes of both the uncorrelated residuals and of the correlation function. Here we use those shapes to extract the joint probability density function. The joint p.d.f. of the observed residuals can be written in terms of ideal, non-correlated residuals and correlation:

$$pdf(res_1^{obs}, res_2^{obs}) = \int pdf(res_1^{unc} - s)pdf(res_2^{unc} - s)pdf(s)ds \tag{2}$$

    Reminding that the residual is function of ID:

$$res = (\mathsf{ID} - <\mathsf{ID}>)\left(\left.\frac{dE}{dx}\right|_{exp-K} - \left.\frac{dE}{dx}\right|_{exp-\pi}\right) = (\mathsf{ID} - <\mathsf{ID}>)\Delta \tag{3}$$

    where we shortened in Δ the difference of expected dE/dx values between kaons and pions — just function of the momentum, we rewrite the joint p.d.f. in terms of ID: $pdf(\mathsf{ID}_1, \mathsf{ID}_2) = pdf[res_1(\mathsf{ID}_1), res_2(\mathsf{ID}_2)]$. We therefore change the variable:

$$pdf(\mathsf{ID}_1, \mathsf{ID}_2) = \int pdf[res_1^{unc}(\mathsf{ID}_1) - s]pdf[res_2^{unc}(\mathsf{ID}_2) - s]\frac{\partial[res_1^{unc}(\mathsf{ID}_1), res_2^{unc}(\mathsf{ID}_2)]}{\partial[\mathsf{ID}_1, \mathsf{ID}_2]}pdf(s)ds$$

    which, expliciting the Jacobian, becomes:

$$pdf(\mathsf{ID}_1, \mathsf{ID}_2) = \int pdf[res_1^{unc}(\mathsf{ID}_1) - s]pdf[res_2^{unc}(\mathsf{ID}_2) - s]\Delta_1\Delta_2 pdf(s)ds \tag{4}$$

From last relation it is clear how we introduced the momentum dependence into the PID-term of the p.d.f. The transformation from residuals to ID leave into the density the differences of expected dE/dx values (Δ), which depend on momentum. Since $\Delta = \Delta(p_1, p_2) \rightarrow \Delta(\alpha, p_{tot})$, therefore $pdf(\mathsf{ID}_1, \mathsf{ID}_2)$, the joint p.d.f. written as a function of ID, becomes $pdf(\mathsf{ID}_1, \mathsf{ID}_2|\alpha, p_{tot})$ and the momentum p.d.f has to be included in the global p.d.f to take into account correctly of the momentum dependence.

– $pdf(\alpha, p_{tot}) = \frac{1}{norm} e^{a_5 p_{tot}} \sum_{i=0}^{4}(a_i, p_{tot}^i) \sum_{j=0}^{6} b_j(\alpha \frac{p_{tot}-2}{p_{tot}-4})^j$ in which the a_i and b_j modes are different for each decay mode. The odd b_j terms are set to zero for the kinematic-symmetric modes $B^0 \rightarrow \pi^+\pi^-$ and $B_s^0 \rightarrow K^+K^-$.

- $\mathcal{L}^{bckg}(\vec{\theta}) = pdf^{mass}(m_{\pi\pi}|\alpha;\vec{\theta}) \cdot pdf^{PID}(\mathsf{ID1}, \mathsf{ID2}|p_{tot}, \alpha; \vec{\theta}) \cdot pdf^{momentum}(\alpha, p_{tot}; \vec{\theta})$ is the background likelihood function.

  – The mass term is parameterised by the sum of an exponential (combinatoric background) and an Argus function (partially, mis-reconstructed B hadrons, like $B \rightarrow \rho K$ and $B \rightarrow \rho\pi$):

$$pdf^{mass}(m_{\pi\pi}|\alpha) = f_{exp} \cdot h_{exp} + f_{ARGUS} \cdot h_{ARGUS}$$

  where $f_{exp} + f_{ARGUS} = 1$ and

$$h_{exp}(m_{\pi\pi}|\alpha) = \frac{1}{Norm} \cdot (e^{(c_1 \cdot m_{\pi\pi})} + c_2)$$

$$h_{\mathrm{ARGUS}}(m_{\pi\pi}|\alpha) = \begin{cases} \frac{1}{Norm} \cdot \left[m_{\pi\pi} \cdot \sqrt{1 - (\frac{m_{\pi\pi}}{m_0})^2} \cdot e^{-c \cdot (\frac{m_{\pi\pi}}{m_0})^2}\right] & \text{if } m_{\pi\pi} < m_0 \\ 0 \text{ if } m_{\pi\pi} > m_0 \end{cases}$$

  In the central fit all parameter of the background mass shape are left free to vary.

  – The parameterisation of the PID likelihood of the background is similar to that used for the signal.We fit the fractions of different particle species: kaons, pions, electrons and protons. The compositions of the two (combinatoric and physics) contributions to the background are fit separately. Since we checked (with a fit) that electron and proton contributions are consistent with zero in the physics (ARGUS) background, we fit this component allowing for the presence of pions and kaons only. In the combinatoric background, instead, we fit independent contributions from electrons, pions, protons, antiprotons, positive kaons, and negative kaons. The fractions of protons and antiprotons are Gaussian-constrained in the fit to the values estimated by the full $B^0 \rightarrow h^+h^{'-}$ fit performed using the complete combined PID, which benefits from the high discriminating power of TOF in separating protons from other particles. The results for the signal fractions and asymmetries from the full-PID fit are very compatible with our central fit, the proton fraction is determined much better and indeed used as a constraint in the central fit.

  – The bidimensional $pdf(\alpha, p_{tot})$ distribution is parameterised with the following function:

$$pdf(\alpha, p_{tot}) = \frac{1}{\text{norm}} \left[1 + \left(\frac{p_{tot} - \lambda}{a}\right)^2\right]^{-m} exp\left[-\nu \ \tan^{-1}\left(\frac{p_{tot} - \lambda}{a}\right)\right] \sum_{j=0}^{6} b_j \ \left(\alpha \ \frac{p_{tot} - 2}{p_{tot} - 4}\right)^j \quad (5)$$

  No asymmetry is expected in the shape of $pdf(\alpha, p_{tot})$ and the odd b_j terms are set to zero.

mode	$\mathcal{M}^2(\alpha) = \mathcal{M}^2(\alpha < 0)$
$B_d \rightarrow \pi^+\pi^-$	$M^2_{B^0_d}$
$B^0_d \rightarrow \pi^- K^+$	$M^2_{B^0_d} + (2+\alpha)(m_\pi^2 - m_K^2)$
$\overline{B}^0_d \rightarrow K^-\pi^+$	$M^2_{B^0_d} + (1 + \frac{1}{1+\alpha})(m_\pi^2 - m_K^2)$
$\overline{B}^0_s \rightarrow \pi^- K^+$	$M^2_{B^0_s} + (2+\alpha)(m_\pi^2 - m_K^2)$
$B^0_s \rightarrow K^-\pi^+$	$M^2_{B^0_s} + (1 + \frac{1}{1+\alpha})(m_\pi^2 - m_K^2)$
$B_s \rightarrow K^+K^-$	$M^2_{B^0_s} + (3 + \alpha + \frac{1}{1+\alpha})(m_\pi^2 - m_K^2)$

mode	$\mathcal{M}^2(\alpha) = \mathcal{M}^2(\alpha > 0)$
$B_d \rightarrow \pi^+\pi^-$	$M^2_{B^0_d}$
$\overline{B}^0_d \rightarrow \pi^+ K^-$	$M^2_{B^0_d} + (2-\alpha)(m_\pi^2 - m_K^2)$
$B^0_d \rightarrow K^+\pi^-$	$M^2_{B^0_d} + (1 + \frac{1}{1-\alpha})(m_\pi^2 - m_K^2)$
$B^0_s \rightarrow \pi^+ K^-$	$M^2_{B^0_s} + (2-\alpha)(m_\pi^2 - m_K^2)$
$\overline{B}^0_s \rightarrow K^+\pi^-$	$M^2_{B^0_s} + (1 + \frac{1}{1-\alpha})(m_\pi^2 - m_K^2)$
$B_s \rightarrow K^+K^-$	$M^2_{B^0_s} + (3 - \alpha + \frac{1}{1-\alpha})(m_\pi^2 - m_K^2)$

TABLE I: Left table: $\mathcal{M}(\alpha)$ for $\alpha < 0$ (i.e. the negative particle carries smaller momentum). Right table: $\alpha > 0$ (i.e. the positive particle carries larger momentum).

Parameter	value
# axial COT SL	$\geq$ 2(5 hits)
# stereo COT SL	$\geq$ 2(5 hits)
# axial SVXII hits	≥ 3
tracking algorithm	sil. r-ϕ and 90°z hits
$\max(\mid\eta(\pi_1)\mid, \mid\eta(\pi_2)\mid)$	≤ 1
$\min(p_T(\pi_1), p_T(\pi_2))$	$\geq$ 2 GeV/c
$p_T(\pi_1)+p_T(\pi_2)$	$\geq$ 5.5 GeV/c
$q(\pi_1)\cdot q(\pi_2)$	< 0
$\Delta\phi(\pi_1,\pi_2)$	$[20°, 135°]$
$\min(\mid d_0(\pi_1)\mid, \mid d_0(\pi_2)\mid)$	$\geq$ 0.0100 cm
$\max(\mid d_0(\pi_1)\mid, \mid d_0(\pi_2)\mid)$	$\leq$ 0.1000 cm
$d_0(\pi_1)\cdot d_0(\pi_2)$	< 0
$\mid\eta(B)\mid$	≤ 1
$\mid d_0(B)\mid$	$\leq$ 0.0080 cm
$L_{xy}(B)$	$\geq$ 0.0300 cm
χ^2_{3D}	7
B isolation	$\geq$ 0.5

Fit parameter	Value
$f(B_d \to \pi\pi)$	0.132±0.014
$f(B_d \to K^{\pm}\pi^{\mp})$	0.621±0.017
$A_{\mathsf{CP}}(B_d \to K^{\pm}\pi^{\mp})$	-0.066±0.039
$f(B_s \to K^{\pm}\pi^{\mp})$	0.027±0.013
$f(B_s \to KK)$	0.220±0.016
$\frac{N(B_s\to KK)}{N(B_d\to K\pi)}$	0.354±0.032
$\frac{N(B_d\to \pi\pi)}{N(B_d\to K\pi)}$	0.212±0.025
$\frac{N(B_s\to K\pi)}{N(B^0\to K\pi)}$	0.044±0.021

TABLE II: *Top left*: list of cuts applied to extract the $B^0 \to h^+h^{'-}$ signal. *Top right*: fit results with statistical errors.

IV. FIT RESULTS

The fit yields the results reported in Tab. II(*top right*).
To convert the value of A_{CP} determined by the fit we need to take into account the relative efficiency of the detector to reconstruct the $B^0 \to K^+\pi^-$ and $\overline{B}^0 \to K^-\pi^+$ decays, due to the larger K^- interaction cross section with the material with respect to K^+. The corrected value is

$$A_{CP}(B^0 \to K^+\pi^-) = -0.058 \pm 0.039(stat.)$$

V. SYSTEMATIC UNCERTAINTIES

- *Mass scale.* The central fit is performed by assuming a known global mass scale, in which we assign to the B^0 and B_s^0 masses the preliminary values measured in Run II [4]. Since the mass is one of the information used in separating all the different contributions it is interesting to check how the fit behaves when the mass scale is allowed to float. An additional output parameter Δ was added to the fit in the parameterization of the input masses: $m^{\rm fit}_{B_s^0} = m^{\rm CDFII}_{B_s^0} + \Delta$ and $m^{\rm fit}_{B^0} = m^{\rm CDFII}_{B^0} + \Delta$ and the global scale of masses is determined to be: 1.7 ± 1.2 MeV/c^2. Then, we generated an ensemble of pseudo-experiments in which the global mass scale is shifted by the above measured value, and we applied the fit to these toy-MC. The observed average systematics on the direct CP asymmetry is of order 0.002.

- *Mass resolution.* In our fit we fixed the relative normalization between the two Gaussians contributing to the mass-distribution of each mode to be 9:1. We assigned a systematic uncertainty to this assumption by repeating the fit on two ensembles of pseudo-experiments, one in which the generated mass-shape is a single Gaussian, the other in which we doubled the size of the additional Gaussian component (20%). The corresponding systematics is order 0.002.

- *Asymmetries in p.d.f.(α, p_{tot}).* In order to take into account hidden asymmetries in the distributions of the probability densities for symmetric modes and background, we repeated the fit after refitting the templates with asymmetric fit functions. The results of the global fit done with these templates varies by 0.0003.

- *dE/dx induced systematics.* We have repeated the global fit by varying the parameters associated to dE/dx calibrations within a 1σ-radius multidimensional sphere in the space of the parameters of the dE/dx calibrations. The resulting systematics is 0.005.

- *Input masses.* The B masses are an input parameter to the fit through the analytic expressions of $\mathcal{M}(\alpha)$. We generated distinct ensembles of pseudo-experiments in which we independently varied the B^0 and B$_s^0$ input masses within $\pm 1\sigma$ statistical uncertainty of the soon to be published CDF II measurement [4] to evaluate the systematics due to the uncertainty on the input masses. The corresponding systematics on the raw CP asymmetry is order 0.0025.

Combinatorial-background model: The central fit uses an exponential distribution for the combinatorial background. We repeated the fit on large ensembles of pseudo-experiments using polynomial distributions (third degree maximum) for the combinatorial background. The resulting systematics is 0.0019.

- *Monte Carlo statistics.* This is the uncertainty deriving from the limited statistics of the Monte Carlo samples used to estimate the relative efficiencies. The statistic uncertainty on the relative efficiencies is 0.001, which results in a 0.001 systematics.

- *Charge Asymmetry.* Since we took the charge asymmetry estimate from the published $D^0 \to h^+ h^{'-}$ analysis [5], we accordingly considered an associated systematic uncertainty whose size is $\pm$ 25% of the difference between corrected and uncorrected asymmetry that corresponds to a order 0.002 change of the asymmetry.

- *Non factorazibility between $m_{\pi\pi}$ and p_{tot}.* A non-perfect factorizability is observed between the two discriminating fit variables $m_{\pi\pi}$ and p_{tot} *i.e.* the mass shape of the background depends slightly on the scalar sum of momenta. We observe a $\sim$ 32% difference between the $m_{\pi\pi}$ slopes observed in events with $p_{\mathrm{tot}} < 9$ GeV$/c$ and in events with $p_{\mathrm{tot}} < 9$ GeV$/c$. A systematic uncertainty on this effect is assessed by repeating the central fit with the background shape fixed respectively to the two slopes observed for $p_{\mathrm{tot}} > 9$ GeV$/c$ and $p_{\mathrm{tot}} < 9$ GeV$/c$. The results of this fit on the asymmetry are order 0.002.

mass scale	0.0022
mass resolution	0.0024
asymmetric momentum-p.d.f	0.0003
dE/dx	0.0050
input masses	0.0025
combinatorial background model	0.0019
p spectra of background	0.0005
MC statistics	0.0010
charge asymmetry	0.0022
$m_{\pi\pi} - p_{tot}$ non factorizability	0.0018
TOTAL (sum in quadrature)	**$\pm$0.0074**

TABLE III: Summary of the systematic uncertainties on the measurement of $A_{CP}(B^0 \to K^+\pi^-)$.

VI. RESULTS

We measured the direct CP asymmetry of $B^0 \to K^+\pi^-$ decays using the first 360 pb^{-1} of data to be:

$$A_{\mathsf{CP}}(B^0 \to K^+\pi^-) = -0.058 \pm 0.039\ (stat.) \pm 0.007\ (syst.) \tag{6}$$

This results is 1.5σ different from zero and can be compared with current world-best measurement from B-factories: $A_{\mathsf{CP}}(B^0 \to K^+\pi^-)_{\mathrm{Babar}} = -0.133 \pm 0.030 \pm 0.009$ [6] and $A_{\mathsf{CP}}(B^0 \to K^+\pi^-)_{\mathrm{Belle}} = -0.113 \pm 0.022 \pm 0.008$ [7] and with the current world-average $A_{\mathsf{CP}}(B^0 \to K^+\pi^-)_{\mathrm{WA}} = -0.115 \pm 0.018$ [8]. Although the statistical resolution of current CDF result is not yet competitive with the B-factories, we have a smaller systematic uncertainty. This is very encouraging in view of the next iteration of the analysis, in which we expect less than 2.5% statistical uncertainty in the 1 fb^{-1} sample already on tape.

Acknowledgments

We thank the Fermilab staff and the technical staffs of the participating institutions for their vital contributions. This work was supported by the U.S. Department of Energy and National Science Foundation; the Italian Istituto Nazionale di Fisica Nucleare; the Ministry of Education, Culture, Sports, Science and Technology of Japan; the Natural Sciences and Engineering Research Council of Canada; the National Science Council of the Republic of China; the Swiss National Science Foundation; the A.P. Sloan Foundation; the Bundesministerium fuer Bildung und

Forschung, Germany; the Korean Science and Engineering Foundation and the Korean Research Foundation; the Particle Physics and Astronomy Research Council and the Royal Society, UK; the Russian Foundation for Basic Research; the Comision Interministerial de Ciencia y Tecnologia, Spain; and in part by the European Community's Human Potential Programme under contract HPRN-CT-20002, Probe for New Physics.

[1] D. Tonelli, the CDF II Collaboration, Prospects in CP Violation at the Tevatron Collider, Pub. Proceedings 18th Les Rencontres De Physique De La Vallee D'Aoste, La Thuile, Aosta Valley, Italy, Feb. 29-March 6, 2004

[2] F. Abe, et al., Nucl. Instrum. Methods Phys. Res. A **271**, 387 (1988); D. Amidei, et al., Nucl. Instum. Methods Phys. Res. A **350**, 73 (1994); F. Abe, et al., Phys. Rev. D **52**, 4784 (1995); P. Azzi, et al., Nucl. Instrum. Methods Phys. Res. A **360**, 137 (1995); The CDF II Detector Technical Design Report, Fermilab-Pub-96/390-E

[3] M. Mangano and M. Cacciari, private communication.

[4] CDF collaboration Measurement of b hadron masses in exclusive J/ψ decays with the CDF detector, hep-ex/0508022.

[5] CDF collaboration, Measurement of Partial Widths and Search for Direct CP Violation in D^0 Meson Decays to K^-K^+ and $\pi^-\pi^+$ PRL 94,122001 (2005).

[6] BaBar collaboration, PRL 93,131801(2004)

[7] Belle collaboration, hep-ex/0507045

[8] Heavy Flavor Averaging Group (April 2006), `www.slac.stanford.edu/xorg/hfag/`

variable	cut value
# axial COT SL	≥ 2(5 hits)
# stereo COT SL	≥ 2(5 hits)
# $r-\phi$ SVXII hits	≥ 3
tracking algorithm	sil. r-ϕ and 90°z hits
$\mid \eta \mid$	$\leq$1
p_T	$\geq$ 2 GeV/c
$p_T(1) + p_T(2)$	$\geq$ 5.5 GeV/c
$q(1) \cdot q(2)$	< 0
$\Delta\phi$	$\geq$20°
$\Delta\phi$	$\leq$135°
$\mid d_0 \mid$	$\geq$100 μm
$\mid d_0 \mid$	$\leq$ 1 mm
$d_0(1) \cdot d_0(2)$	<0 cm^2

TABLE IV: Track selection.

variable	cut value
$\mid \eta \mid$	$\leq$ 1
$\mid d_0 \mid$	$\leq$ 80 μm
L_{xy}	$\geq$ 300 μm
χ^2_{3D}	$\leq$ 7
isolation $I_{R=1}$	$\geq$ 0.5

TABLE V: Candidate selection.

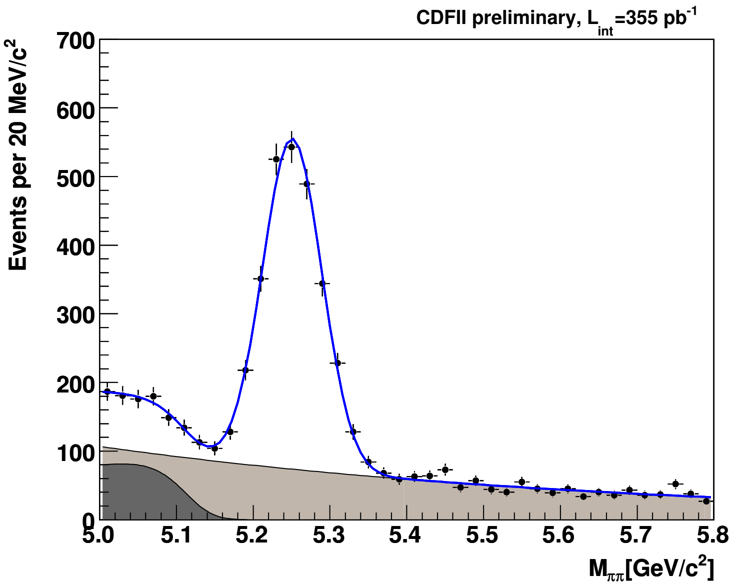

FIG. 1: Invariant $\pi\pi$-mass distribution obtained after applying the optimized analysis cuts reported in table II. A Gaussian (signal) plus exponential (combinatoric background) plus a smeared Argus (physics background) fit function is overlaid.

parameter	fraction	yield
$B^0 \to \pi^+\pi^-$ + c.c.	(0.132 ± 0.014)	313 ± 34
$B^0 \to K^+\pi^-$ + c.c.	(0.621 ± 0.017)	1475 ± 60
$A_{\mathsf{CP}}(B^0 \to K^+\pi^-)$	(-0.066± 0.039)	–
$B^0_s \to K^-\pi^+$ + c.c.	(0.027 ± 0.013)	64 ± 30
$B^0_s \to K^+K^-$ + c.c.	(0.220 ± 0.016)	523 ± 41

TABLE VI: Raw physics results from the fit. By "raw" we mean that the numbers have not been corrected for the relative efficiency factors yet.

parameter	value
$\frac{1}{2}(f_{\pi^+} + f_{\pi^-})$ (combinatorial)	0.517 ± 0.017
$\frac{1}{2}(f_{e^+} + f_{e^-})$ (combinatorial)	0.022 ± 0.005
f_p (combinatorial)	0.230 ± 0.017
$f_{\bar{p}}$ (combinatorial)	0.273 ± 0.018
$\frac{1}{2}(f_{K^+} + f_{K^-})$ (combinatorial)	0.209 ± 0.022
fraction of physics bckg (ARGUS norm.)	0.162 ± 0.020
ARGUS cut-off [GeV/c^2]	5.118 ± 0.001
ARGUS shape	28 ± 7
f_π (ARGUS)	0.688 ± 0.046
f_K (ARGUS)	0.312 ± 0.046
background fraction	0.552 ± 0.013
c_1 (background shape)	-1.34 ± 0.17
σ_1 *primary* gaussian [MeV/c^2]	23.7 ± 1.0
σ_2 *secondary* gaussian [MeV/c^2]	64 ± 21

TABLE VII: Raw complementary results from the fit. By "raw" we mean that the numbers have not been corrected for the relative efficiency factors yet.

source	shift wrt central fit
mass scale	0.0022
mass resolution	0.0024
asymmetric momentum-p.d.f	0.0003
dE/dx	0.0050
input masses	0.0025
combinatorial background model	0.0019
p **spectra of background**	0.0005
MC statistics	0.0010
charge asymmetry	0.0022
$\boldsymbol{m_{\pi\pi} - p_{tot}}$ **non-factorizability**	0.0018
TOTAL (sum in quadrature)	**0.0074**

TABLE VIII: Summary of systematic uncertainties.

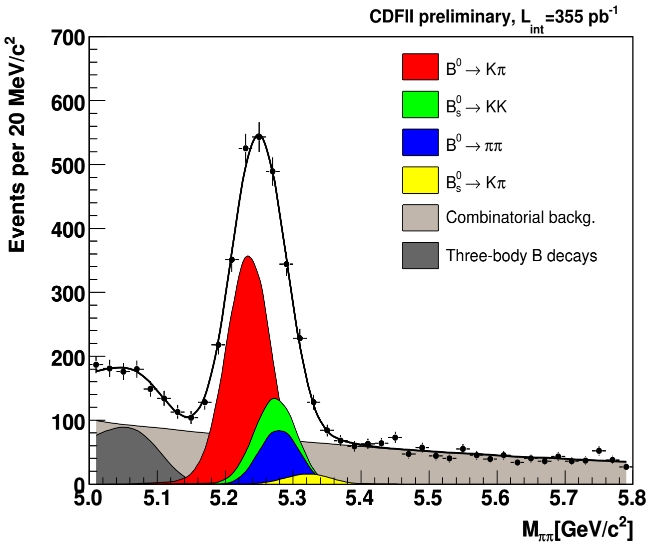

FIG. 2: Fit projections onto the $m_{\pi\pi}$ variable.

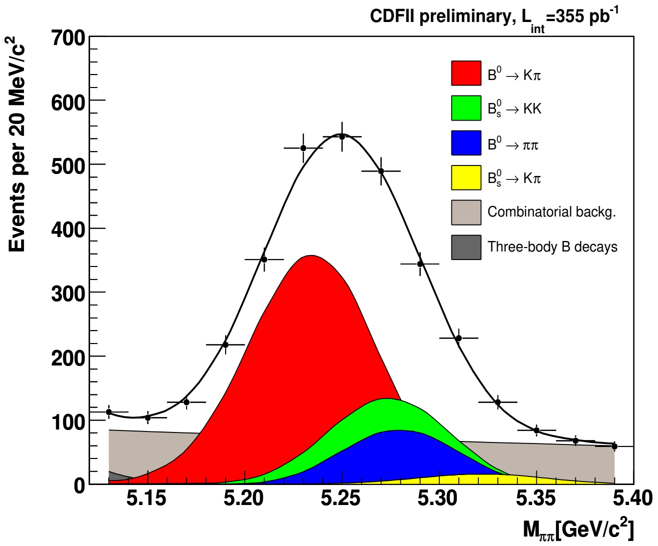

FIG. 3: Fit projections onto the $m_{\pi\pi}$ variable expanded in the signal region.

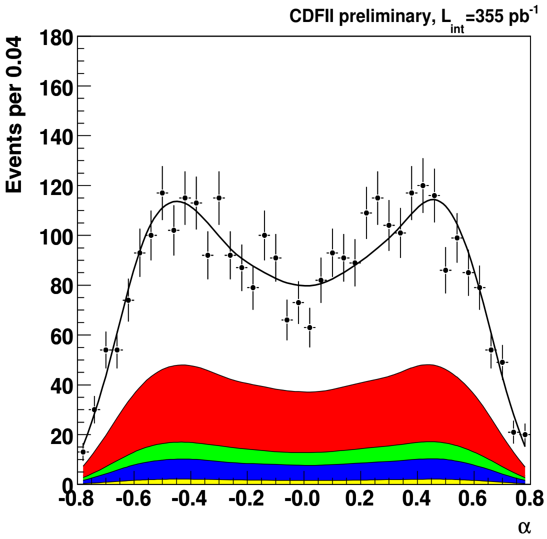

FIG. 4: Fit projections onto the α variable of events in the signal region.

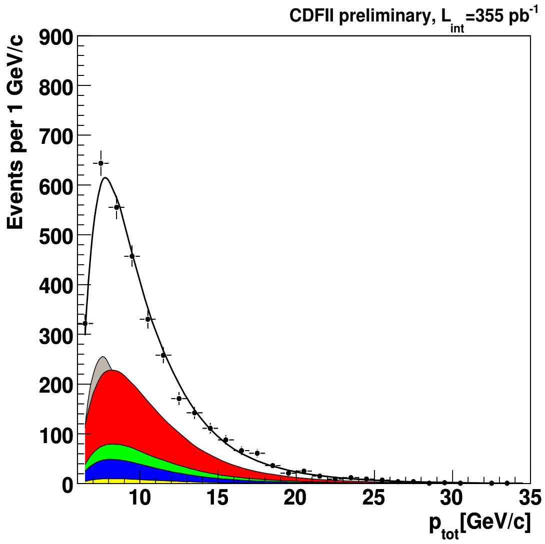

FIG. 5: Fit projections onto the p_{tot} variable of events in the signal region.

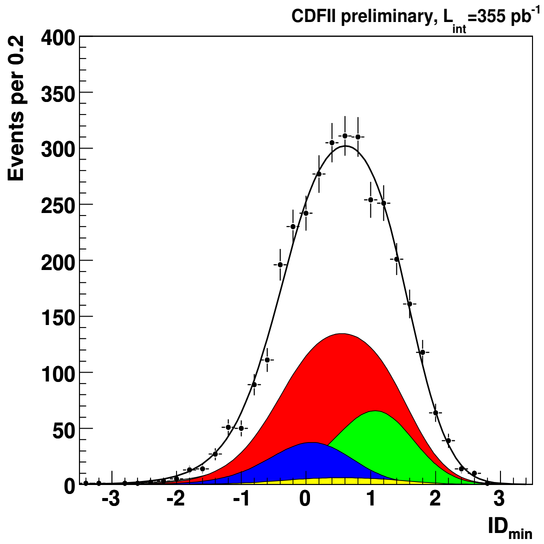

FIG. 6: Fit projections onto the ID_1 variable of events in the signal region.

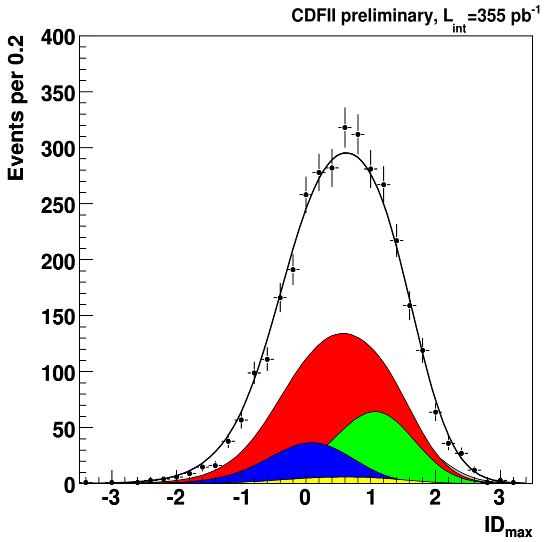

FIG. 7: Fit projections onto the ID_2 variable of events in the signal region.

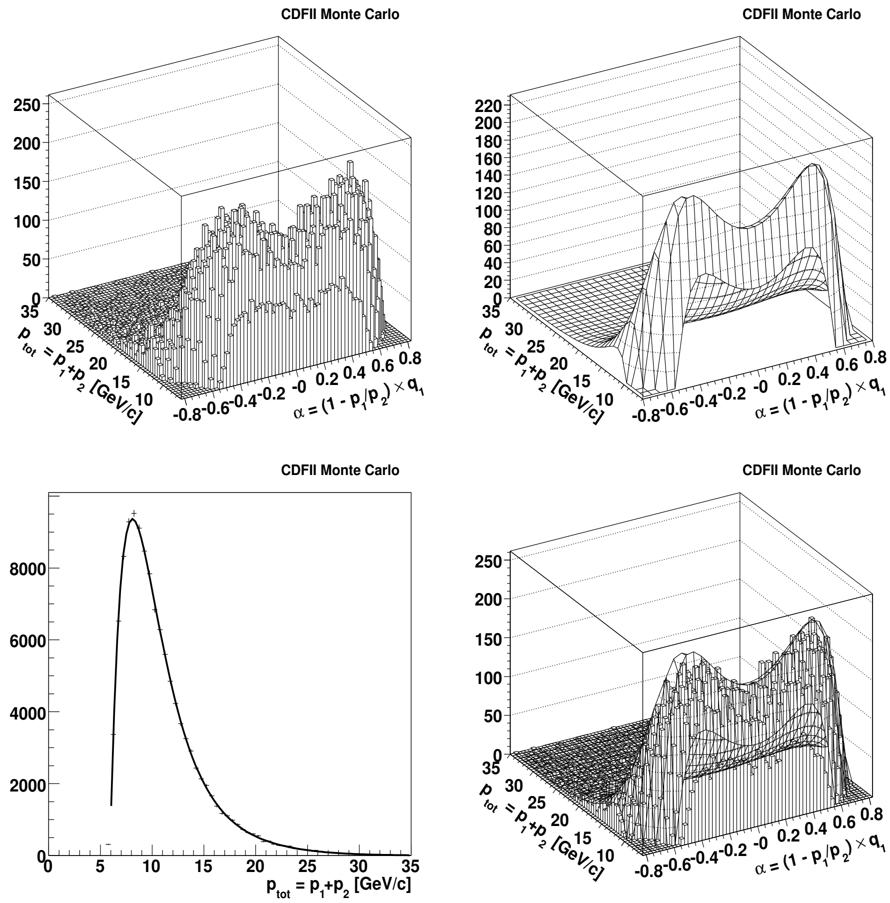

FIG. 8: Determination of the joint (α, p_{tot}) density for the mode $B^0 \to \pi^+\pi^-$. Top left plot: distribution of $\alpha - p_{tot}$ in simulated events. Top right plot: fit results. Bottom left plot: result of the fit of the p_{tot} distribution. Bottom right plot: result of the two-dimensional fit overlaid to the distribution of Monte Carlo.

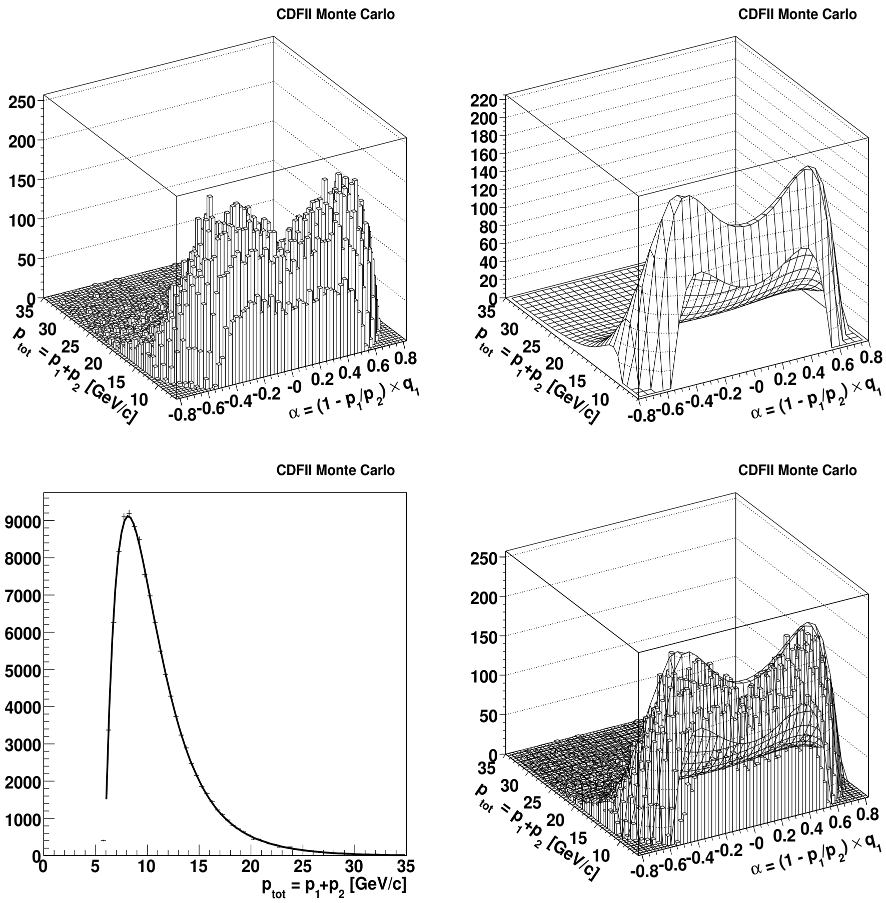

FIG. 9: Determination of the joint (α, p_{tot}) density for the mode $B^0 \to K^+\pi^-$. Top left plot: distribution of $\alpha - p_{tot}$ in simulated events. Top right plot: fit results. Bottom left plot: result of the fit of the p_{tot} distribution. Bottom right plot: result of the two-dimensional fit overlaid to the distribution of Monte Carlo.

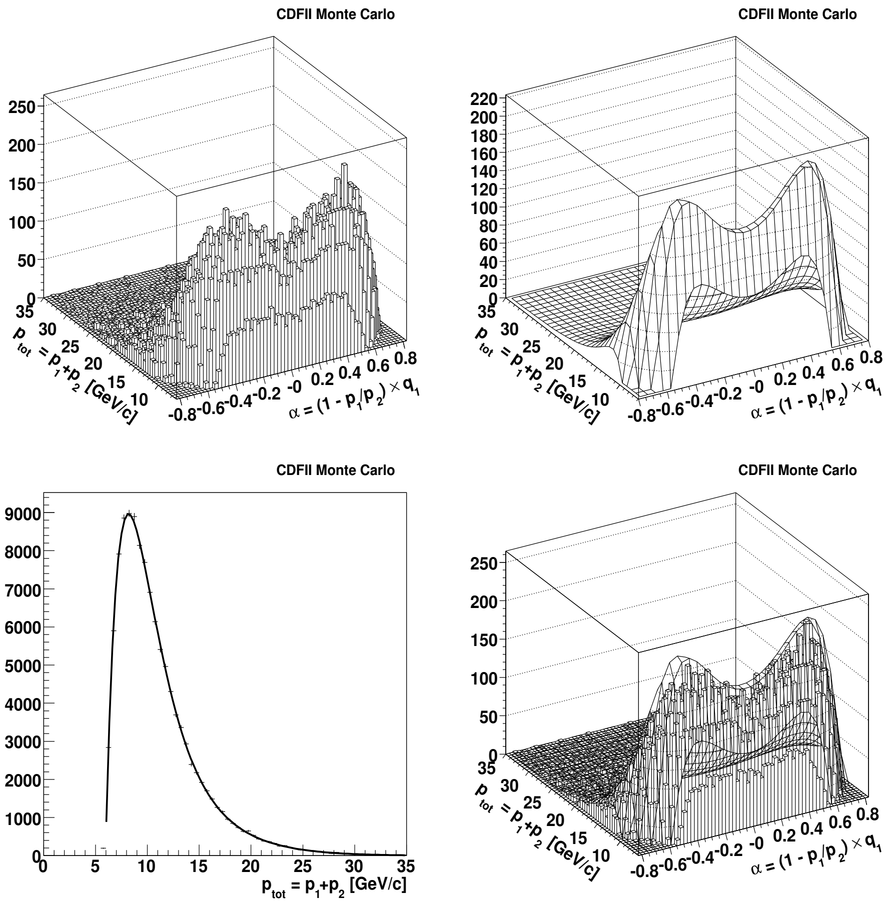

FIG. 10: Determination of the joint (α, p_{tot}) density for the mode $B_s^0 \to K^-\pi^+$. Top left plot: distribution of $\alpha - p_{tot}$ in simulated events. Top right plot: fit results. Bottom left plot: result of the fit of the p_{tot} distribution. Bottom right plot: result of the two-dimensional fit overlaid to the distribution of Monte Carlo.

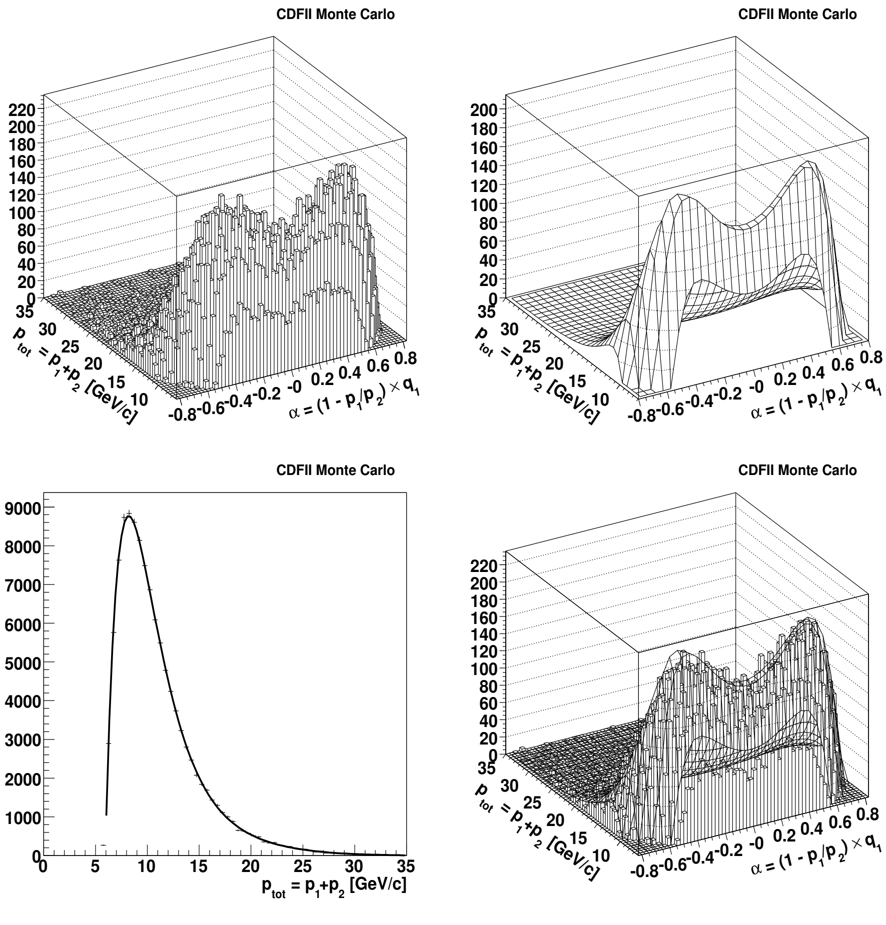

FIG. 11: Determination of the joint (α, p_{tot}) density for the mode $B_s^0 \to K^+K^-$. Top left plot: distribution of $\alpha - p_{tot}$ in simulated events. Top right plot: fit results. Bottom left plot: result of the fit of the p_{tot} distribution. Bottom right plot: result of the two-dimensional fit overlaid to the distribution of Monte Carlo.

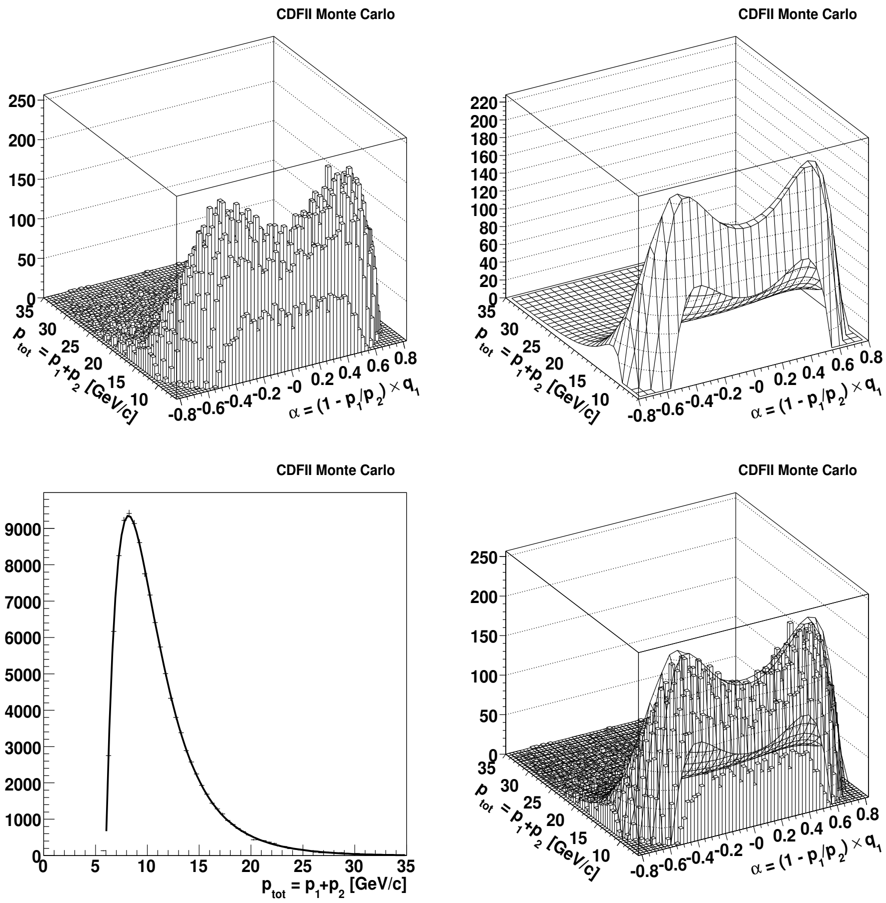

FIG. 12: Determination of the joint (α, p_{tot}) density for the mode $B_s^0 \to \pi^+\pi^-$. Top left plot: distribution of $\alpha - p_{tot}$ in simulated events. Top right plot: fit results. Bottom left plot: result of the fit of the p_{tot} distribution. Bottom right plot: result of the two-dimensional fit overlaid to the distribution of Monte Carlo.

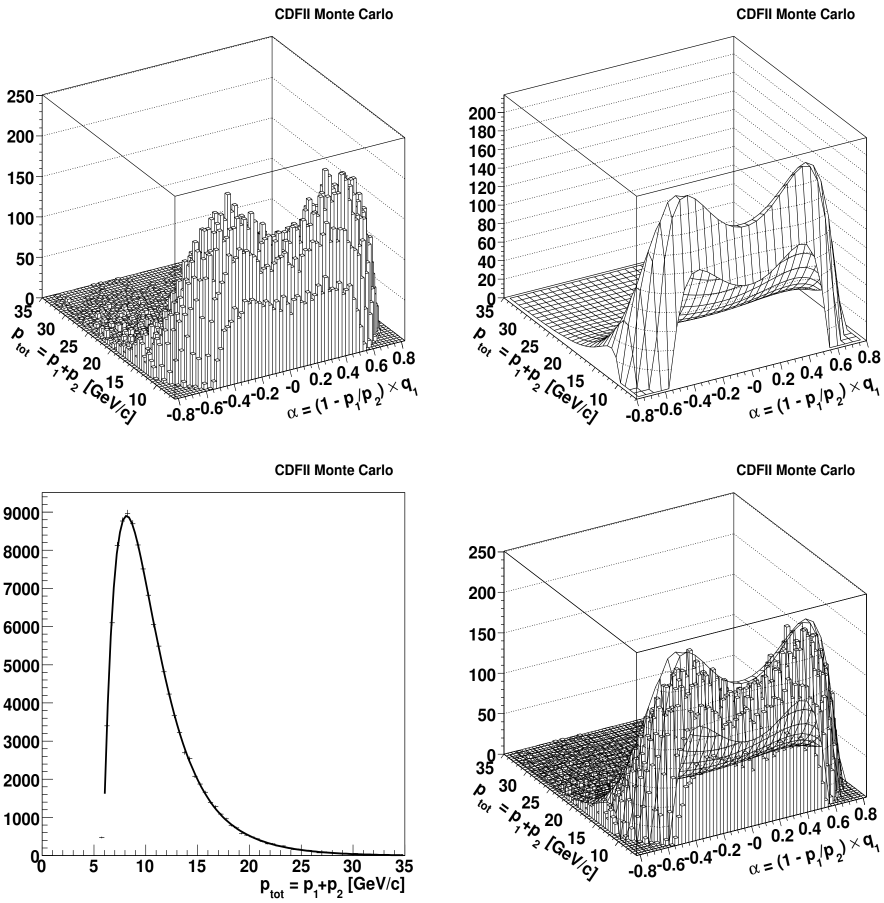

FIG. 13: Determination of the joint (α, p_{tot}) density for the mode $B^0 \to K^+K^-$. Top left plot: distribution of $\alpha - p_{tot}$ in simulated events. Top right plot: fit results. Bottom left plot: result of the fit of the p_{tot} distribution. Bottom right plot: result of the two-dimensional fit overlaid to the distribution of Monte Carlo.

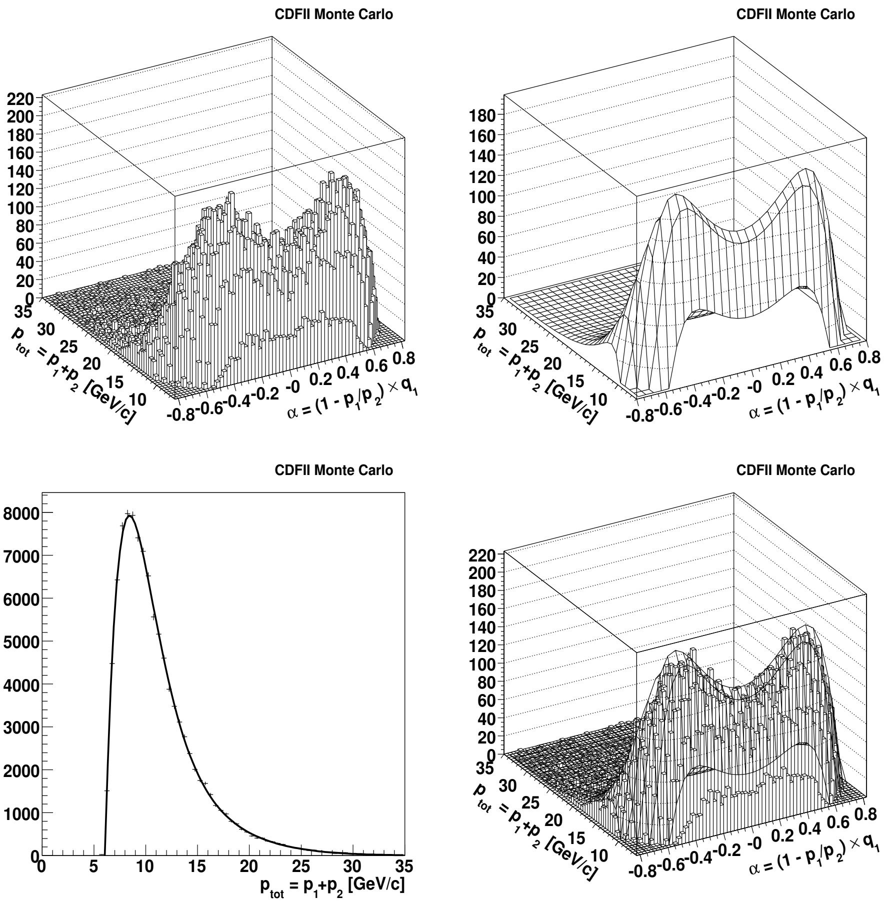

FIG. 14: Determination of the joint (α, p_{tot}) density for the mode $\Lambda_b^0 \to p\pi^-$. Top left plot: distribution of $\alpha - p_{tot}$ in simulated events. Top right plot: fit results. Bottom left plot: result of the fit of the p_{tot} distribution. Bottom right plot: result of the two-dimensional fit overlaid to the distribution of Monte Carlo.

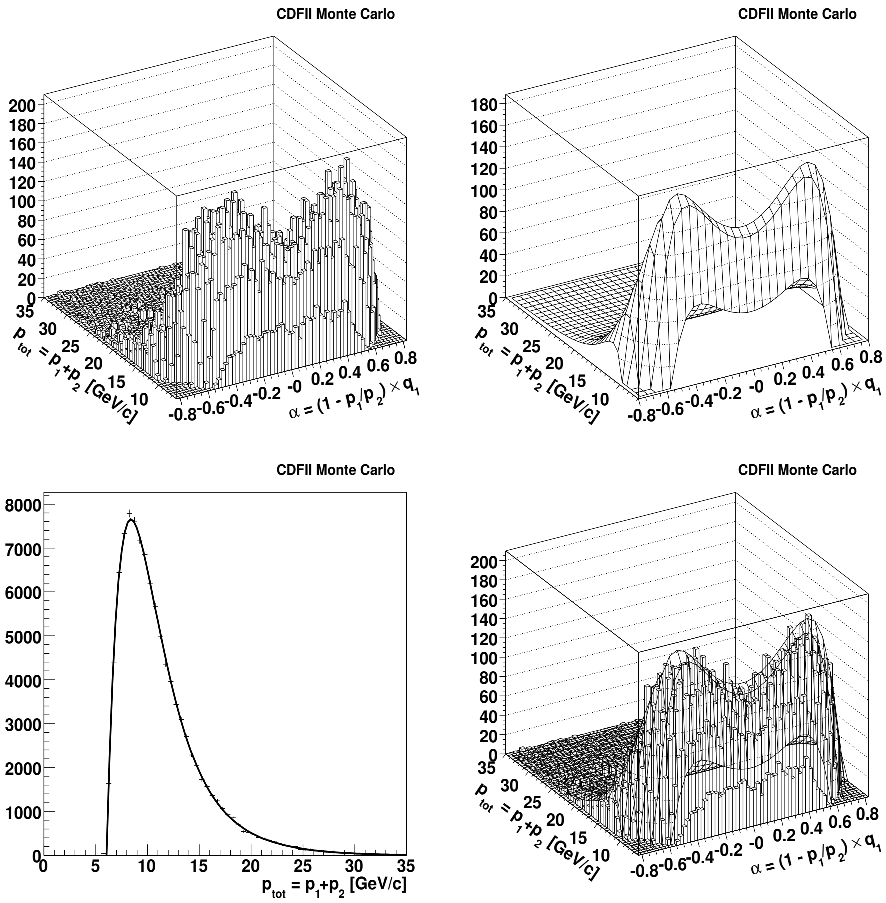

FIG. 15: Determination of the joint (α, p_{tot}) density for the mode $\Lambda_b^0 \to pK^-$. Top left plot: distribution of $\alpha - p_{tot}$ in simulated events. Top right plot: fit results. Bottom left plot: result of the fit of the p_{tot} distribution. Bottom right plot: result of the two-dimensional fit overlaid to the distribution of Monte Carlo.

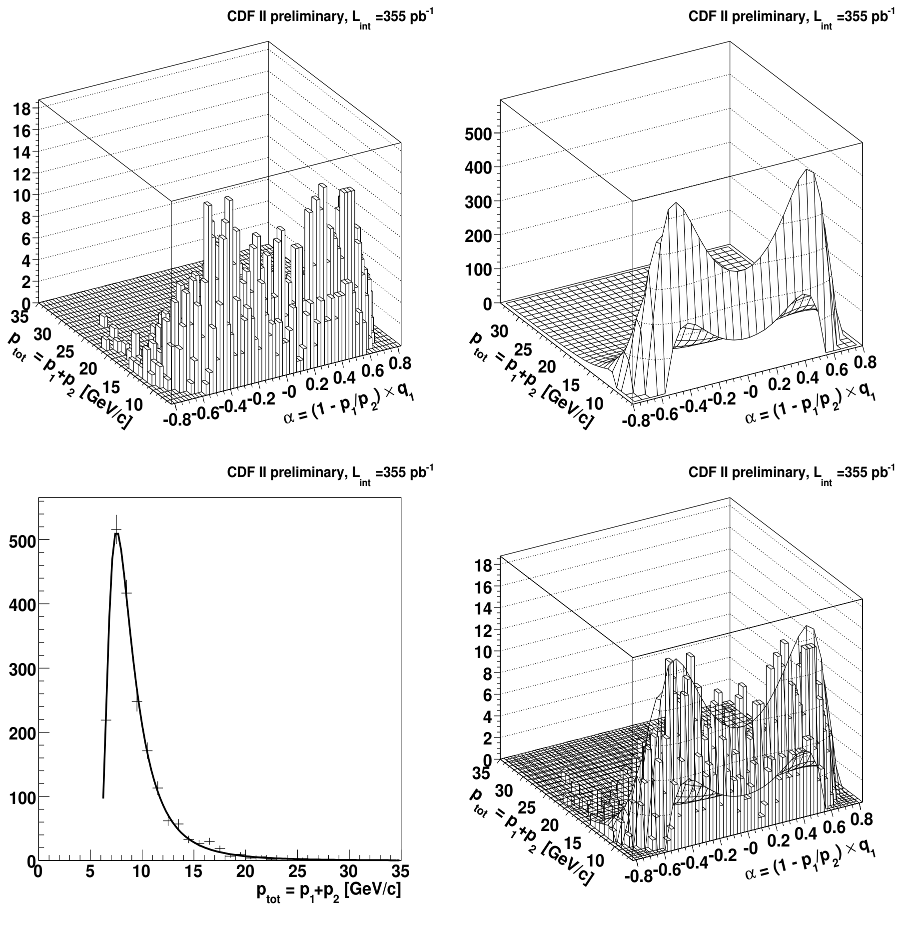

FIG. 16: Determination of the joint (α, p_{tot}) density for background. Top left plot: distribution of $\alpha - p_{tot}$ in simulated events. Top right plot: fit results. Bottom left plot: result of the fit of the p_{tot} distribution. Bottom right plot: result of the two-dimensional fit overlaid to the distribution of data.